Supporting Information

Self-Assembly of a Covalent Organic Cage with Exceptionally Large and Symmetrical Interior Cavity: The Role of Entropy of Symmetry

Paweł Skowronek, Beata Warżajtis, Urszula Rychlewska*, Jacek Gawroński*

Exceptionally large size cuboctahedral imine cage is obtained from small size organic molecules in a thermodynamically driven [8+12] cyclocondensation. This is a demonstration of the role of entropy of symmetry as a driving force in reversible reactions.

Mastalerz (M. Mastalerz, *Chem. Commun.*, 2008, 4756-4758; M. Mastalerz, M. W. Schneider, I. M. Oppel, O. Presly, *Angew. Chem. Int. Ed.*, 2011, **50**, 1046-1051) used 4-*tert*-butyl-2,6-diformylphenol (**1**) for condensation with 2,7,14-triaminotriptycene to obtain a T_d symmetry adamantanoid nanocapsule, in a yield (58%) significantly lower than in other cases. In this nanocapsule all salicyldiimine moieties adopt the *syn*, *anti* conformation. According to our calculations, this is indeed the most stable of the three possible conformers of a model *bis*-*N*-methylimine derivative of **1** (Scheme S1). The persistency of the *syn*, *anti* conformation of the salicyldiimine moiety in cage molecules was tested by us in a condensation of **1** with other tritopic amines. Calculations performed for a condensation product of **1** and *cis*,*cis*-1,3,5-triaminocyclohexane (**2**) revealed that in order to obtain a cage of T_d symmetry, the salicyldiimine moiety would have to adopt an energetically less favorable *syn*, *syn* conformation, thus adding significant steric energy (4.9 kcal mol^{-1} per salicyldiimine unit) to the structure. Therefore the formation of a higher O_h symmetry cage was anticipated in the reaction of **1** and **2**, in order to keep *syn*, *anti* conformation of the salicyldiimine moiety unchanged.

Scheme S1 Possible conformers of *bis*-*N*-methylimine of 2,6-diformylphenol and their relative energies (kcal mol^{-1}) calculated at the (MP2/6-311G(d,p)//B3LYP/6-311G(d,p) level

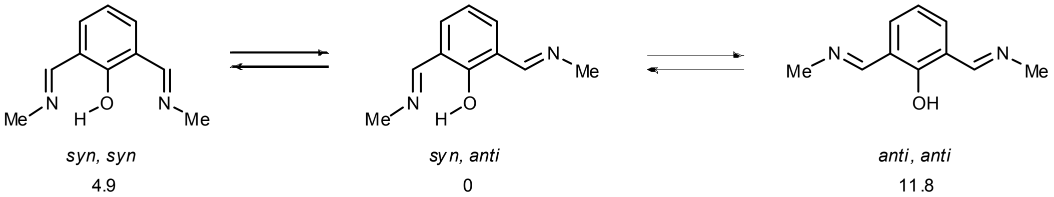

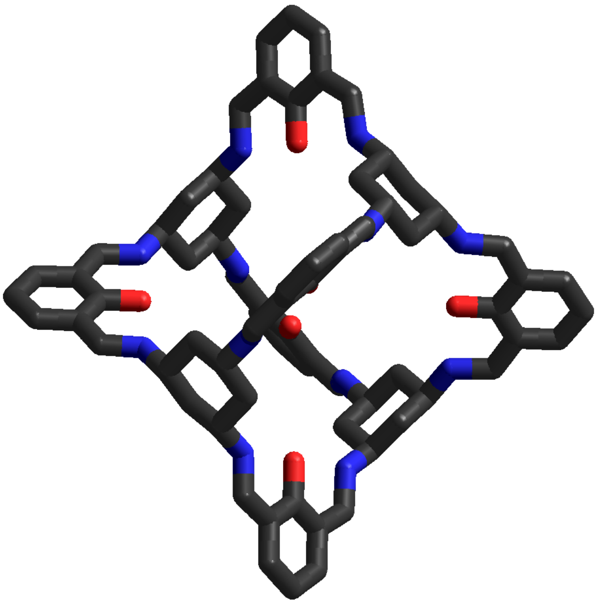

Theoretical tetrahedral product of condensation of 4-tert-butyl-2,6-diformylphenol **1** and cis,cis-1,3,5-triaminocyclohexane **2**. Hydrogen atoms are omitted for clarity.

Experimental

Synthesis of cage **3** was performed by mixing solutions of triamine **2** (72 mg, 0.56 mmol) in a mixture of CH_2Cl_2 (4 ml) and MeOH (3 ml) and dialdehyde **1** (172 mg, 0.83 mmol) in CH_2Cl_2 (4 ml). After 24 h at room temperature clear solution was evaporated at low temperature and obtained solid was analyzed. ^1H NMR (300 MHz, $CDCl_3/CD_3OD$) δ 8.98 (s, 1H), 8.46 (s, 1H), 8.13 (d, J = 2.4 Hz, 1H), 7.35 (d, 1H), 7.32 (m, 1H). 3.8-3.6 (m, 1H), 3.6-3.45 (m, 1H), 2.4-1.7 (m, 4H), 1.33 (s, 9H), ^{13}C NMR (75 MHz, $CDCl_3/CD_3OD$) δ 163.22, 158.93, 156.71, 141.49, 130.94, 127.03, 122.33, 118.28, 69.52, 64.53, 40.89, 34.11, 31.14. IR (KBr) 1683, 1632 cm^{-1}, MALDI-TOF MS M^+3076.122.

Cage **3** was found insoluble neither in CH_2Cl_2 nor in MeOH alone but soluble in their mixture. Other popular solvents did not dissolve cage **3**. Heating in solution (>80°C) or prolonged storage led to decomposition of the compound (see TGA curve Figure S10).

Crystals grown from a mixture of methanol and dichloromethane were very unstable and turned opaque within minutes upon removal from their mother liquor. Therefore, the crystal selected for X-ray analysis was frozen in a perfluoroalkane matrix cooled by a nitrogen stream. This was already an indication that substantial amounts of loosely bound solvent molecules are present in the crystal lattice. The powder X-ray diffraction pattern (PXRD) of the sample taken from the mother liquor (crushed opaque crystals) showed a limited degree of crystallinity and did not match the pattern simulated from the single crystal structure (Fig. S9). X-ray intensities for both powder and single crystal samples were collected on an Oxford Diffraction SuperNova Atlas Dual system with a (Cu) microfocus source and focusing multilayer mirror optics. The data resolution was estimated, based on a $I>2\sigma(I)$ criterion, as approximately 1.1 Å. The structure was solved by direct methods using SHELXS-86 program[1] and refined by full matrix least squares using SHELXL-86.[1] All non-hydrogen atoms were refined using anisotropic thermal parameters. The positions of the hydrogen atoms were calculated and refined in a so called 'riding model' with the isotropic displacement parameters 20% higher than the isotropic equivalent of the displacement parameter of the atom to which the hydrogen atom was bonded. Low scattering power of the crystal enabled us to locate only three of the highly disordered water molecules belonging to the first hydration sphere of the molecule. These were the water molecules that act as fasteners of the cage construction. The remaining solvent molecules could not be easily located and refined. Therefore, we have corrected the observed data by using the SQUEEZE routine in PLATON.[2] We have found 2927 electrons in 9080 A^3, which means that around 53% of the unit cell is filled with disordered solvent molecules. After that we were able to refine the structure to R values of R1=0.076 and wR2 (all data)=0.240. Atomic coordinates have been deposited at the Cambridge Crystallographic Data Centre (CCDC 909668).

Crystal Data: T=100(5) K, $C_{192}H_{240}N_{24}O_{12} \cdot 12H_2O$, M=3292.08, tetragonal, space group $P\bar{4}2_1c$, a=b=25.7826(5) Å, c=25.6888(7) Å, V=17076.4(7) $Å^3$, Z=2, Dx=0.640 gcm^{-3}, reflections collected/unique 61966/6726 [R(int)=0.074], data/restrains/parameters 6726/151/505 GOF 1.02, final $R[I>2\sigma(I)]$ R_1=0.076, wR_2 (all data)=0.240, residual density 0.24 eA^{-3}.

1 G. M. Sheldrick, *Acta Cryst*. **2008**, *A64*, 112-122.
2 A. L. Spek, *Acta Cryst*. **2009**, *D65*, 148-155.

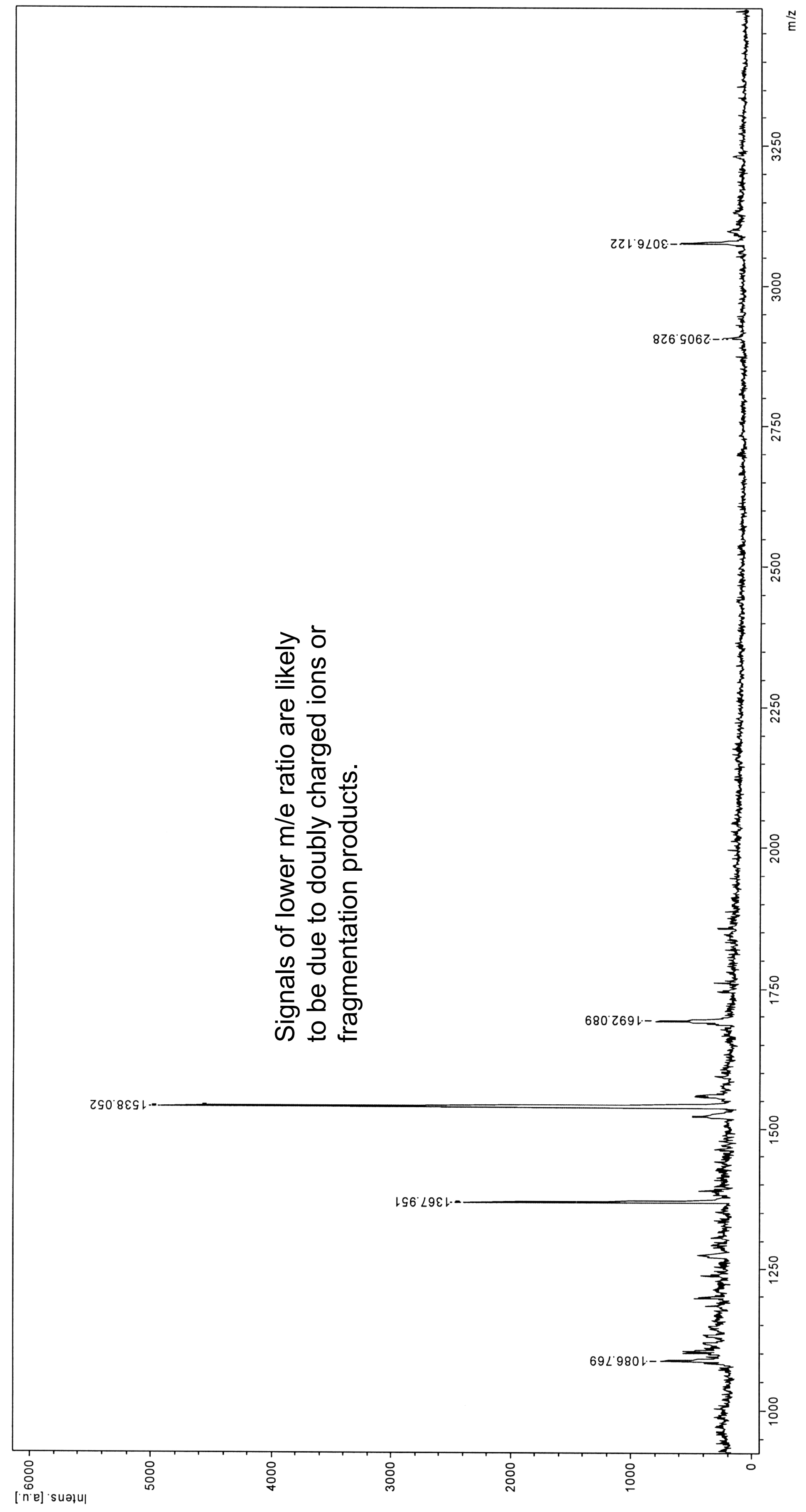

Signals of lower m/e ratio are likely to be due to doubly charged ions or fragmentation products.

Figure S1. MALDI-TOF MS spectrum of cage 3

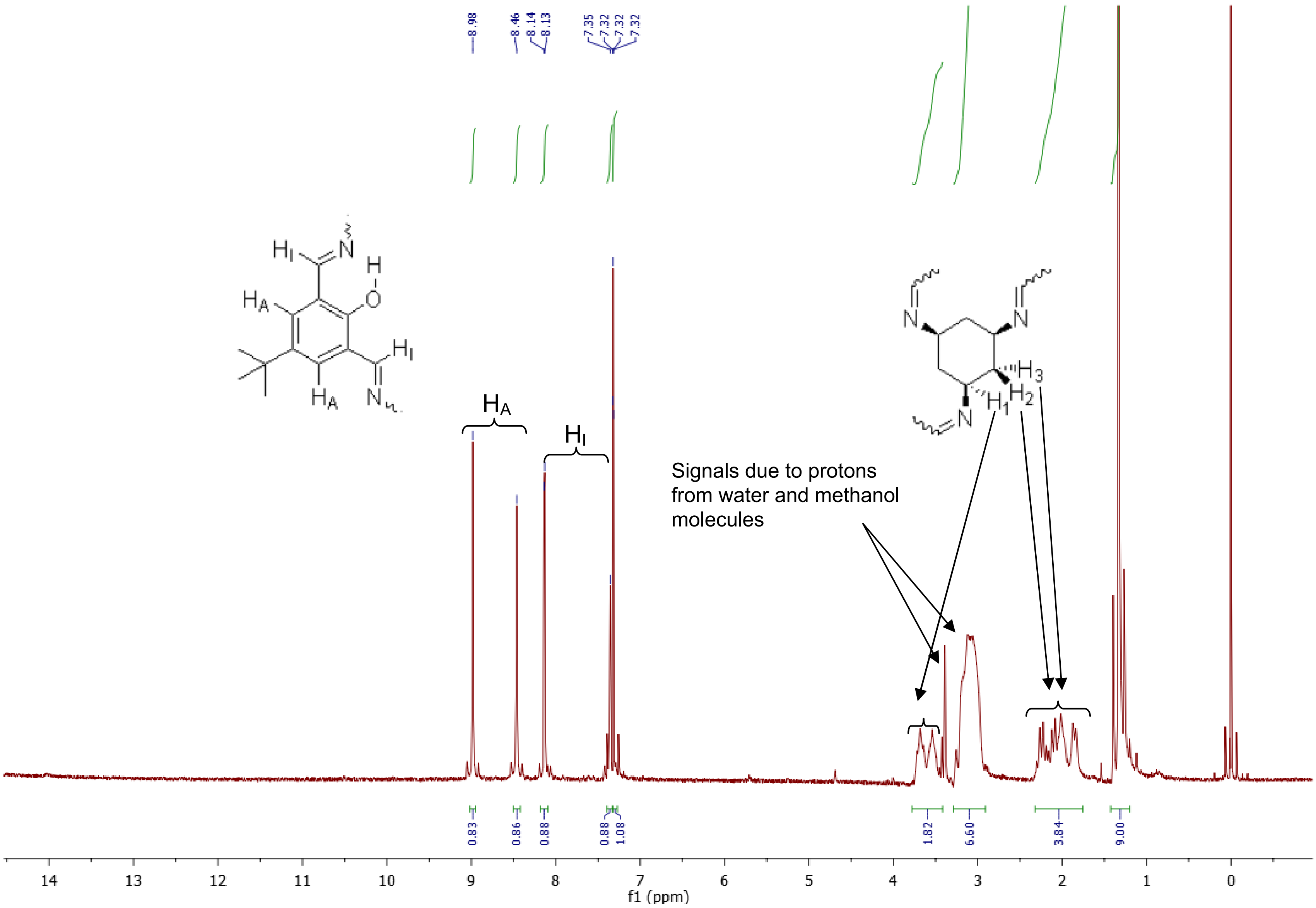

Signals due to protons from water and methanol molecules

Figure S2. ^{1}H NMR spectrum of crude cage **3**.

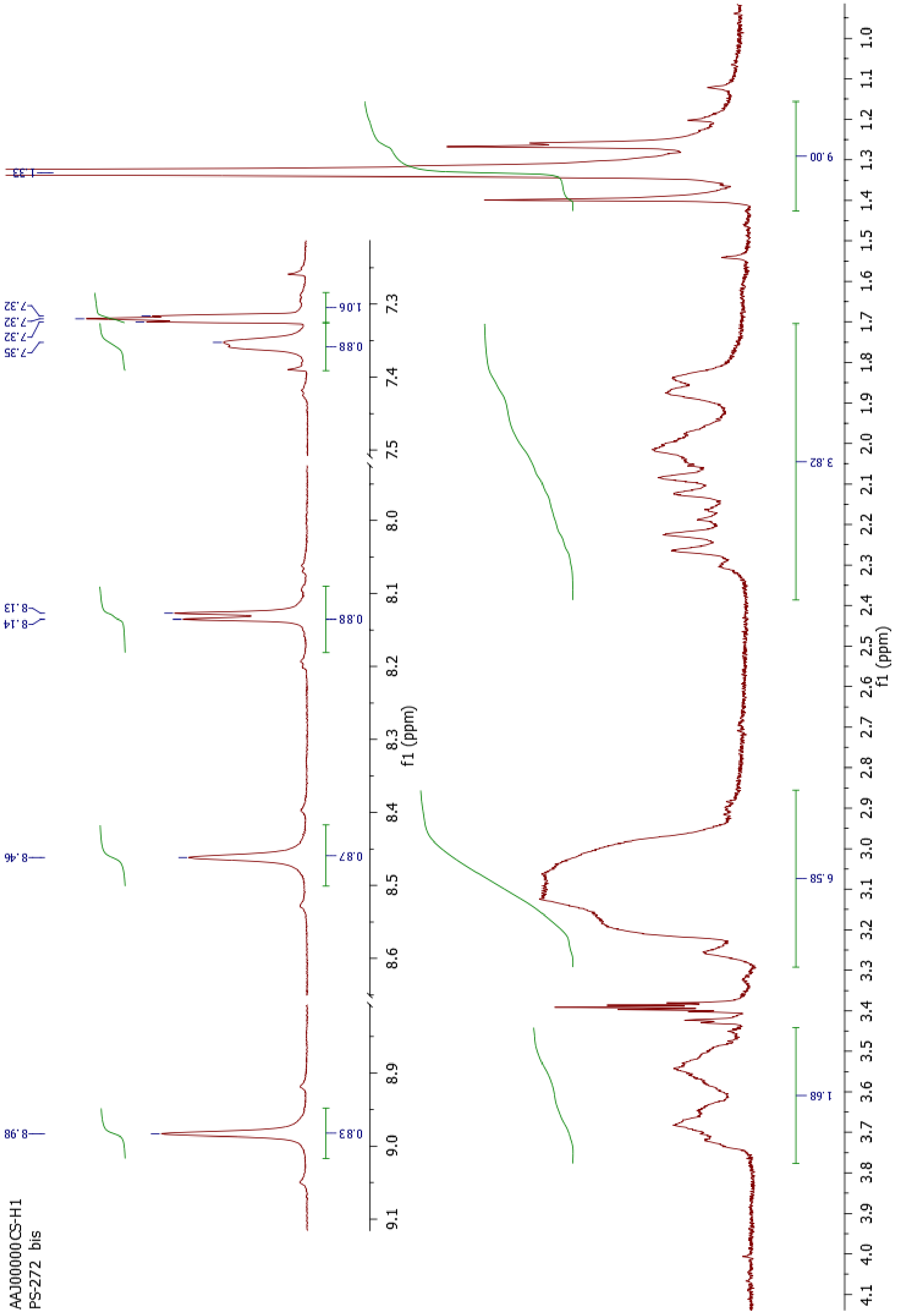

Figure S3. Extensions of ^{1}H NMR spectrum of crude cage **3**.

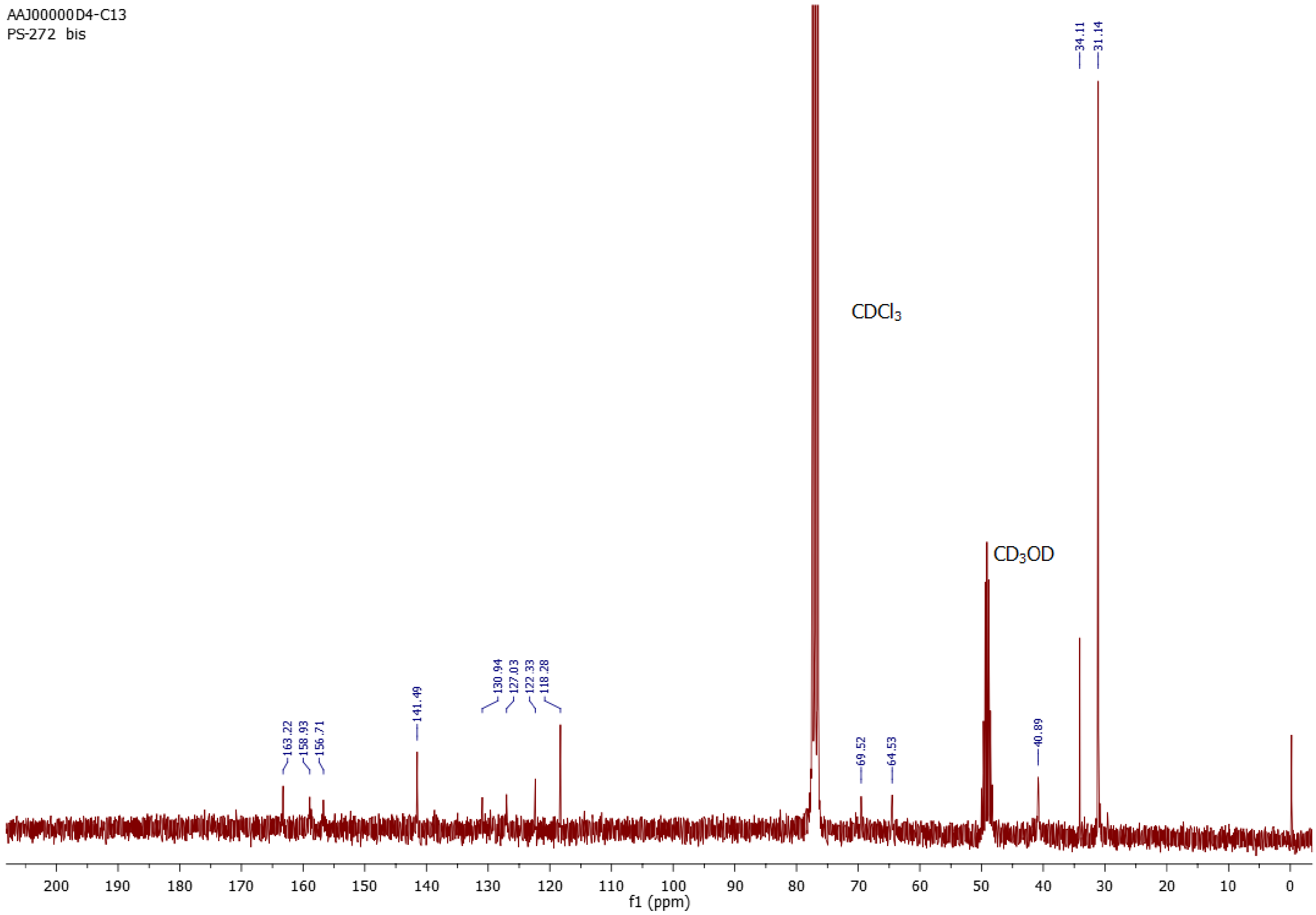

Figure S4. ^{13}C NMR spectrum of crude cage **3**.

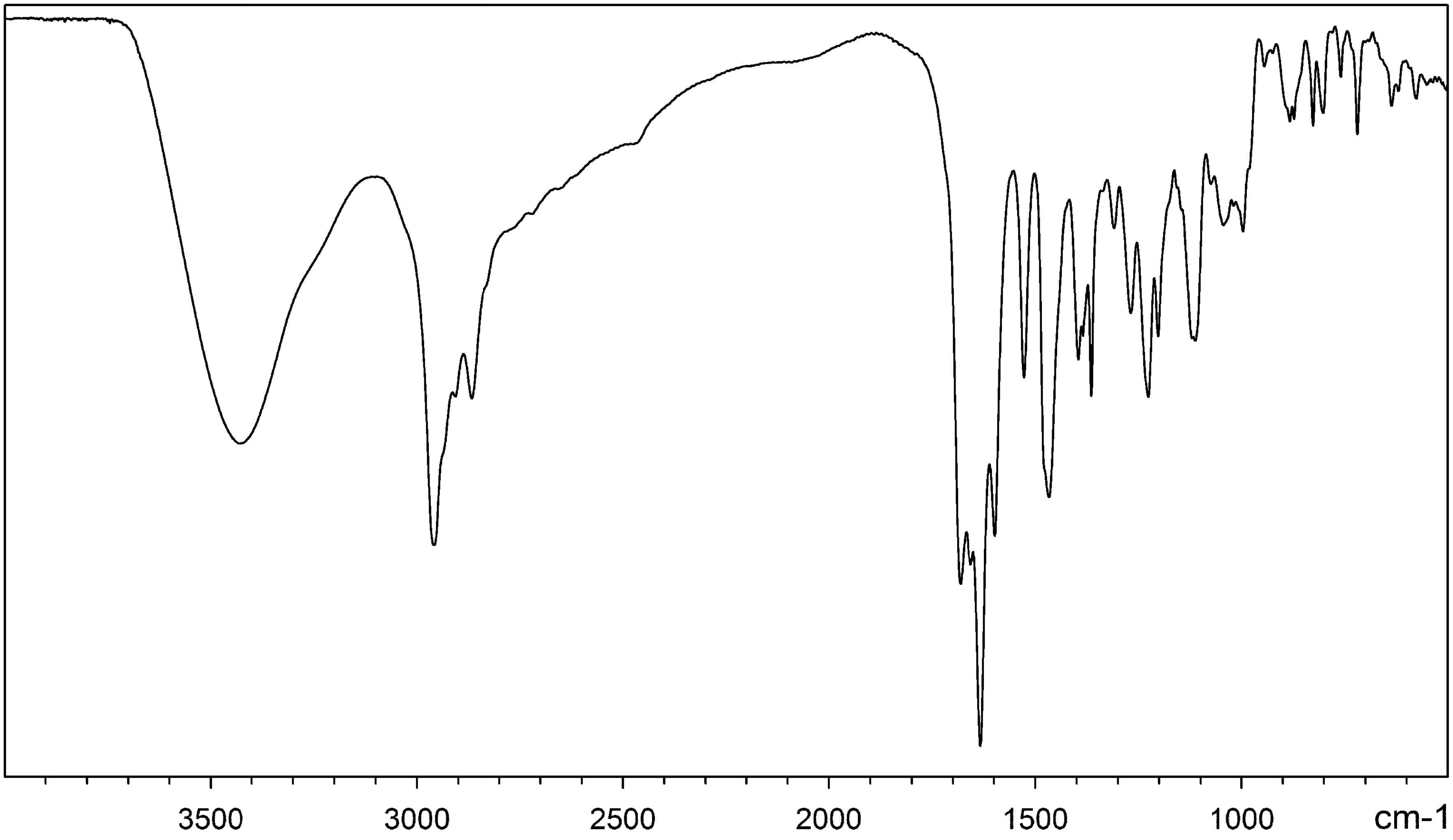

Figure S2. IR spectrum of crude cage **3**.

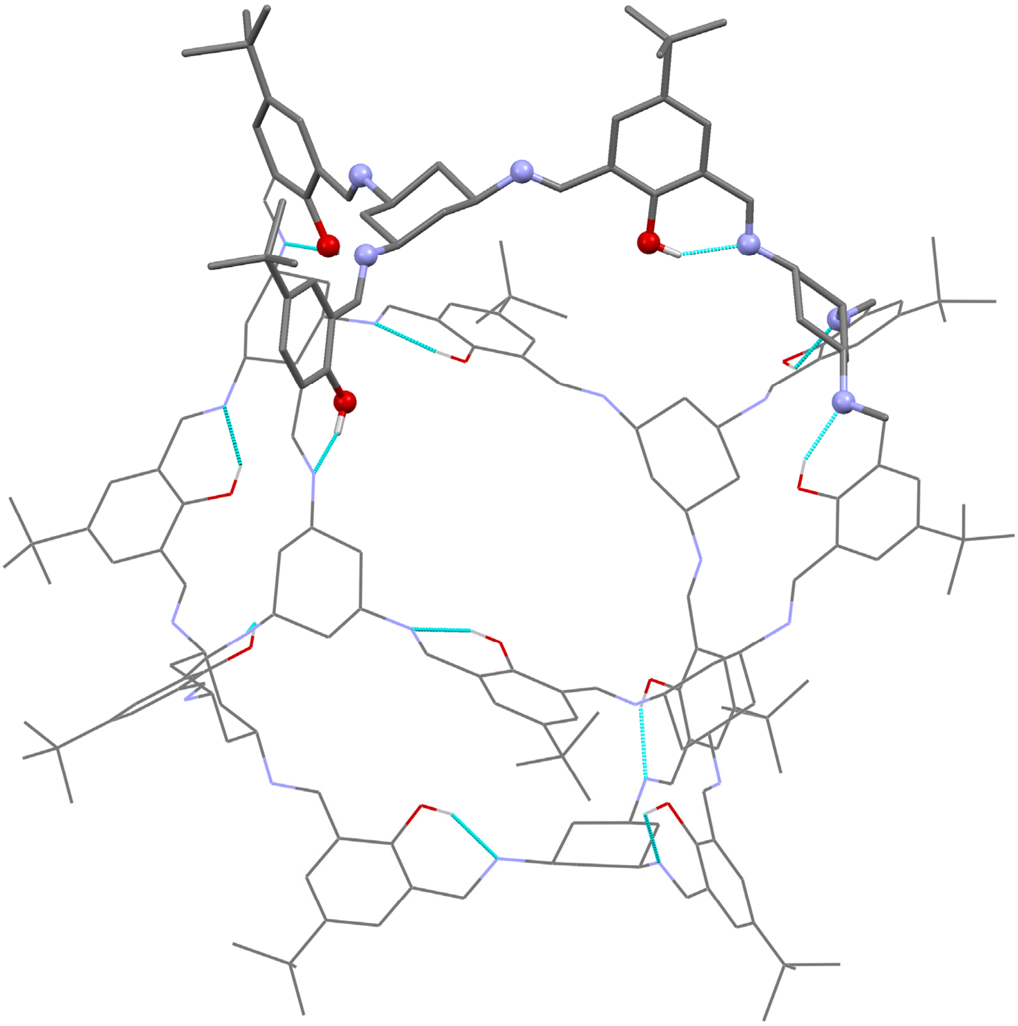

Figure S6. Molecular conformation adopted in the solid state. Note the alternate syn and anti orientation of the C=N bonds with respect to the hydroxy substituent and formation of intramolecular O-H•••N hydrogen bonds. H-atoms not involved in hydrogen bonding are omitted.

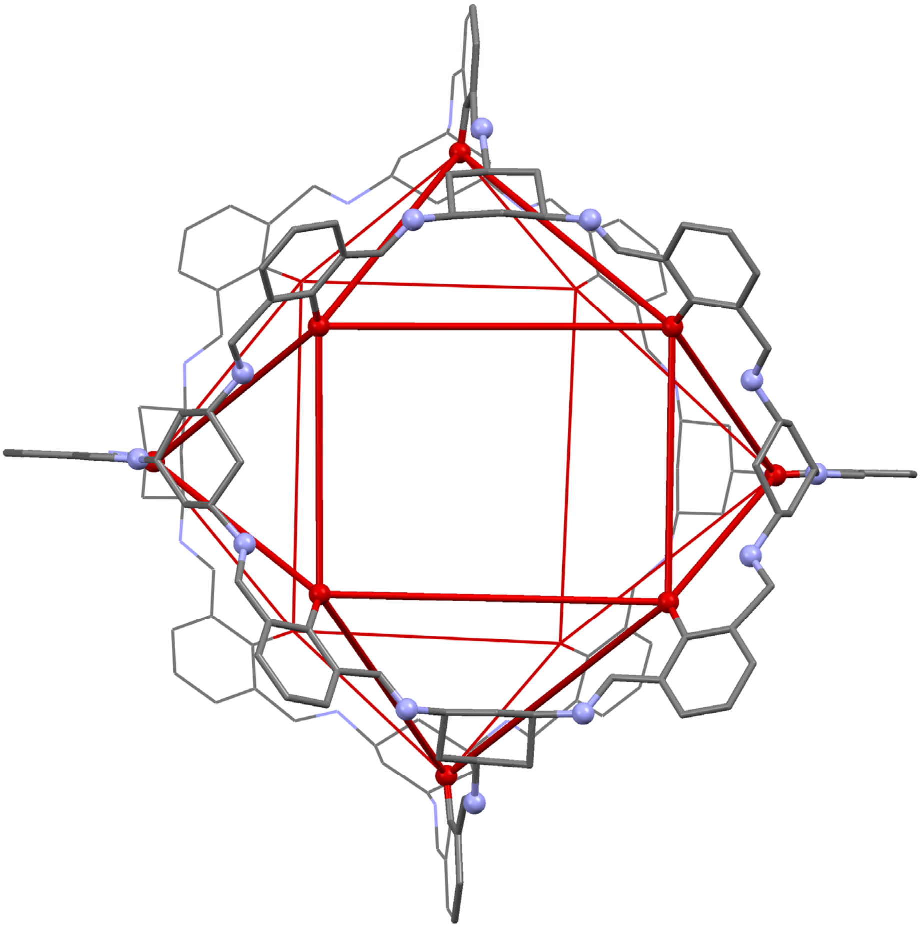

Figure S7. Cubooctahedral O_{12} structural unit viewed along approximate fourfold axis displays the entrance to the macromolecular cavity from one of the six {100} faces of the cuboctahedron. The terminal *tert*-butyl groups and hydrogen atoms have been omitted for clarity.

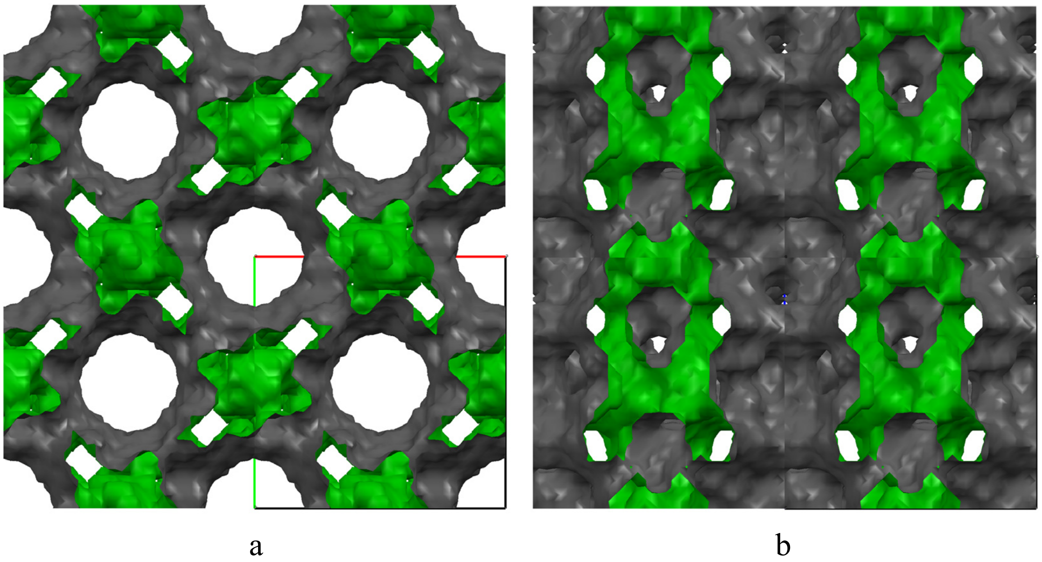

Figure S8 a, b) Intra- and intermolecular solvent accessible voids in the crystal structure of **3** represented as white areas surrounded by black walls viewed along c- and a-direction, respectively.

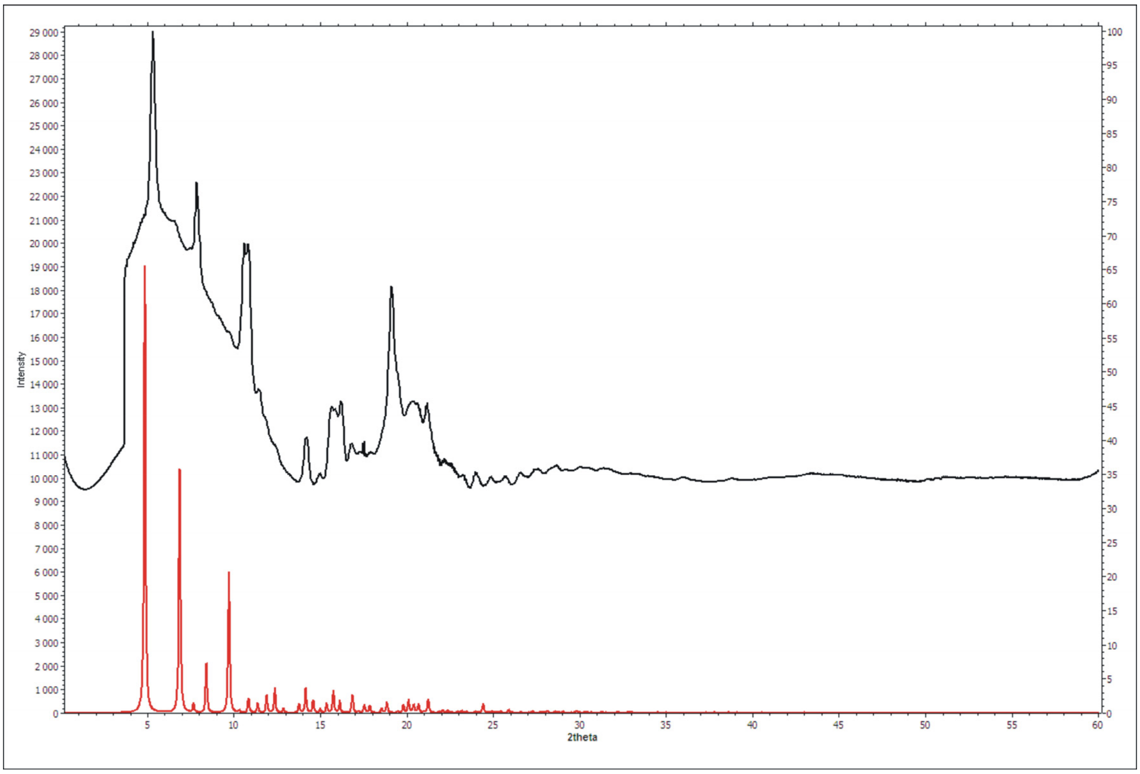

Figure S9 Comparison of experimental XRPD pattern measured at 293K for the crystals taken from the mother liquor (black curve), and the simulated pattern from the single-crystal determination at 100K (red curve).

Table S1. Selected hydrogen-bond parameters

D—H···*A*	*D*—H (Å)	H···*A* (Å)	*D*···*A* (Å)	*D*—H···*A* (°)
O9—H9···N1	0.84	1.87	2.616 (6)	148
O29—H29···N2^{i}	0.84	2.03	2.587 (9)	123
O49—H49···N3^{ii}	0.84	1.82	2.573 (7)	149
O1w···O2w^{iii}			2.695 (12)	
O1w···O3w^{ii}			2.928 (8)	
O2w···O3w^{iii}			2.516 (16)	

Symmetry code(s): (i) *y*, -*x*+1, -*z*+2; (ii) -*x*+1, -*y*+1, *z*; (iii) -y+1, x, -*z*+2.

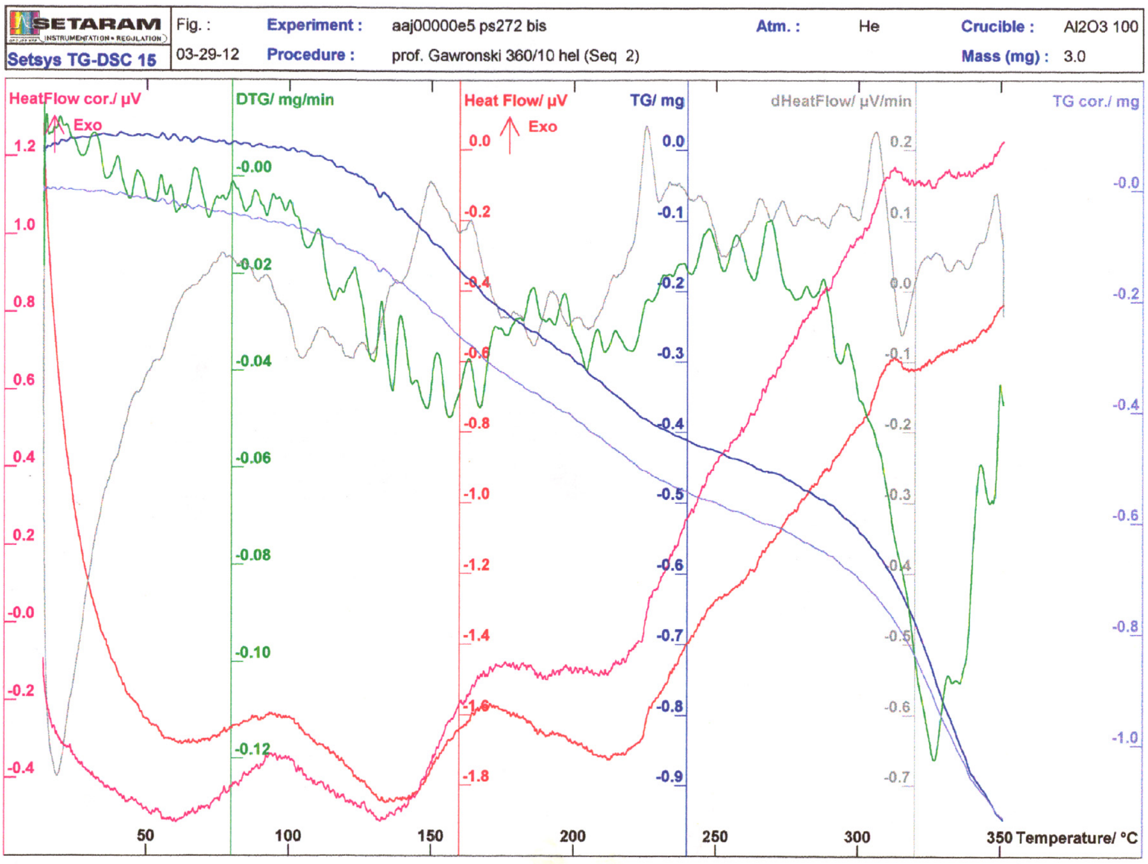

Figure S10. TG analysis of cage **3.**